

Desorption of benzoic and stearic acid adsorbed upon montmorillonites: a thermogravimetric study

Longfei Lu · Ray L. Frost · Jingong Cai

Received: 1 February 2009 / Accepted: 9 March 2009 / Published online: 19 June 2009
© Akadémiai Kiadó, Budapest, Hungary 2009

Abstract The desorption of benzoic acid and stearic acid from sodium and calcium montmorillonites has been studied using thermogravimetric and differential thermogravimetric analysis. Desorption of benzoic acid from sodium montmorillonites occurs at 140 °C and from calcium montmorillonites at 179 °C. This increase in temperature is attributed to the benzoic acid bonding to the calcium in the interlayer. A lowering of the dehydroxylation temperature of montmorillonites is observed with acid adsorption. Stearic acid desorbs at 218 °C as observed by the DTG curves. The desorption pattern differs between the sodium montmorillonites and the calcium montmorillonites.

Keywords Thermogravimetric analysis · Differential thermogravimetric analysis · Montmorillonites · Desorption · Benzoic acid · Stearic acid

Introduction

Clay minerals are the most abundant inorganic minerals in natural systems. The surface properties of colloidal clay particles play the major role in the formation, structure and strength of aggregates in sediments and soils. Sediment organic matter (SOM), mainly polarity organic molecules

such as carboxylic acids, has strong affinity to the surface of clay minerals. Through their interaction by physical or chemical bonds, organoclay complexes are formed. Sorption of SOM is considered to be a major process in the preservation of organic matter (OM) in sediments and soils. Association of OM with minerals provides protection against not only rapid microbial decay but also oxidation. Kennedy et al. [1] provided evidence that SOM was preserved quite well in interlayer of smectite clay in Cretaceous black shale. But the protective effect of clay minerals on pyrogenation of SOM is not well known. The adsorption of acids on clays is important for our understanding of soils [2–4]. Equally important is to understand the adsorption-desorption phenomena [5–7]. If acids such as benzoic acid and stearic acid adsorb on soil containing clays then fundamentally natural organoclays are formed.

Organoclays form an important type of modified clay material. Their uses are many including some environmental applications [8–12]. Organoclays are particularly useful in water purification e.g. by the removal of oil and toxic chemicals from water [10, 13–15]. Remediation of industrial waste waters is enabled through the use of organoclays [16, 17]. These types of materials are useful for the remediation of contaminated soils [18–20] and they are also applied as clay liners in landfills. The development of some new nanocomposite materials is due to use of organoclays [21–24]. Organo-montmorillonites are synthesized by introducing cationic surfactants such as quaternary ammonium compounds into the interlayer space through ion exchange [25–27]. Long-chain alkylammonium cations can form a hydrophobic medium within the clay interlayer, and act in analogy to a bulk organic phase. The intergallery distance of $d(001)$ plane of the clay which has not been organically modified, is relatively small, and the intergallery environment is hydrophilic. Intercalation of an

L. Lu · R. L. Frost (✉)
Inorganic Materials Research Program, School of Physical and Chemical Sciences, Queensland University of Technology,
2 George Street, GPO Box 2434, Brisbane, QLD 4001, Australia
e-mail: r.frost@qut.edu.au

L. Lu · J. Cai
State Key Laboratory of Marine Geology, Tongji University,
Shanghai 200092, China

organic surfactant between the clay layers can not only change the surface properties from hydrophilic to hydrophobic, but also significantly increase the basal spacing of the layers.

The use of thermal analysis techniques to study montmorillonitic clays is well known [28]. Some thermoanalytical studies of organo-modified clays have been forthcoming [29–31]. A recent review has demonstrated the applicability of DTA-TG for differentiating between adsorbed and free organic matter and also between ionic and molecular adsorption [30]. This work has shown that the location of the exothermic peaks is diagnostic and serves to show the adsorption of organic molecules on metallic cations. Many of the thermal analytical studies have been applied to nanocomposites involving organoclays [32]. However there have been almost no studies of the thermal stability of organoclays and no studies of the structure of organoclays. Recently thermal analysis techniques have proven most useful for the study of complex mineral systems [33–39] and materials generated through the modification of surfaces [40–45]. Modification of surfaces through intercalation has also been studied using thermal analysis techniques.

This paper reports the changes in the structure of a montmorillonitic clay with adsorbed-intercalated organic acids. X-ray diffraction and high-resolution thermogravimetric analyses are used to study the changes in the clays basal spacing depending on the adsorption of the benzoic and stearic acids.

Experimental

Materials

The montmorillonite used in this study was supplied by the Clay Minerals Society as source clay SWy-2-Na-Montmorillonite (Wyoming). This clay originates from the Newcastle formation, (cretaceous), County of Crook, State of Wyoming, USA. The cation exchange capacity (CEC) is 76.4 meq/100 g (according to the specification of its producer).

Preparation of acid adsorption on clay

Five grams stearic acid and benzoic acid were dissolved and made up to 250 mL with toluol, respectively. Ten grams Ca or Na montmorillonite were weighted into a 500 mL glass reaction bulb. Two hundred milliliters of the acid solution were pipetted into reaction bulb with a magnetic stir bar. The samples were stirred for 8 h in 35 ± 2 °C. The solids were recovered by centrifugation, washed once with toluol, twice with ethanol, and thereafter

once with acetone. After each washing the solids were separated from the liquid by centrifugation. The product was allowed to dry at room temperature.

X-ray diffraction

X-ray diffraction patterns were collected using a Philips X'pert wide angle X-ray diffractometer, operating in step scan mode, with Cu K $_{\alpha}$ radiation (1.54052 Å). Patterns were collected in the range 3–90° 2 θ with a step size of 0.02° and a rate of 30 s per step. Samples were prepared as a finely pressed powder into aluminium sample holders. The Profile Fitting option of the software uses a model that employs 12 intrinsic parameters to describe the profile, the instrumental aberration and wavelength dependent contributions to the profile.

Thermal analysis

Thermal decomposition of the acid adsorbed on montmorillonite was carried out in a TA[®] Instruments incorporated high-resolution thermogravimetric analyzer (series Q500) in a flowing nitrogen atmosphere (80 cm³/min). Approximately 50 mg of sample was heated in an open platinum crucible at a rate of 2.0 °C/min up to 500 °C. The TGA instrument was coupled to a Balzers (Pfeiffer) mass spectrometer for gas analysis. Only selected gases such as water and carbon dioxide were analyzed.

Results and discussion

X-ray diffraction

Montmorillonite consists of tetrahedral silica layers and octahedral alumina layers, carrying negative charges which must be counterbalanced by exchangeable cations in the interlayers. Such an arrangement results in a basal spacing of around 11.7 Å in an air dry state. This basal spacing is dependent upon the size of the cation be it Na, Ca or Mg and also on the degree of hydration of the cation. This degree of hydration is very dependent on the vapour pressure of water and the temperature.

The XRD patterns of sodium and calcium montmorillonite before and after adsorption of benzoic acid and stearic acid are shown in Fig. 1a–d. The XRD pattern of calcium montmorillonite before and after adsorption of stearic acid and benzoic acid did not vary significantly, except some new peaks at 2 θ value of 8.1°, 16.3°, 23.8° and 25.9° at benzoic acid–calcium montmorillonite complexes attributed to benzoic acid. They all exhibited a sharp diffraction peak at 2 θ value of 5.8°, which corresponded to interlayer distances of 15.29 Å. The diffraction

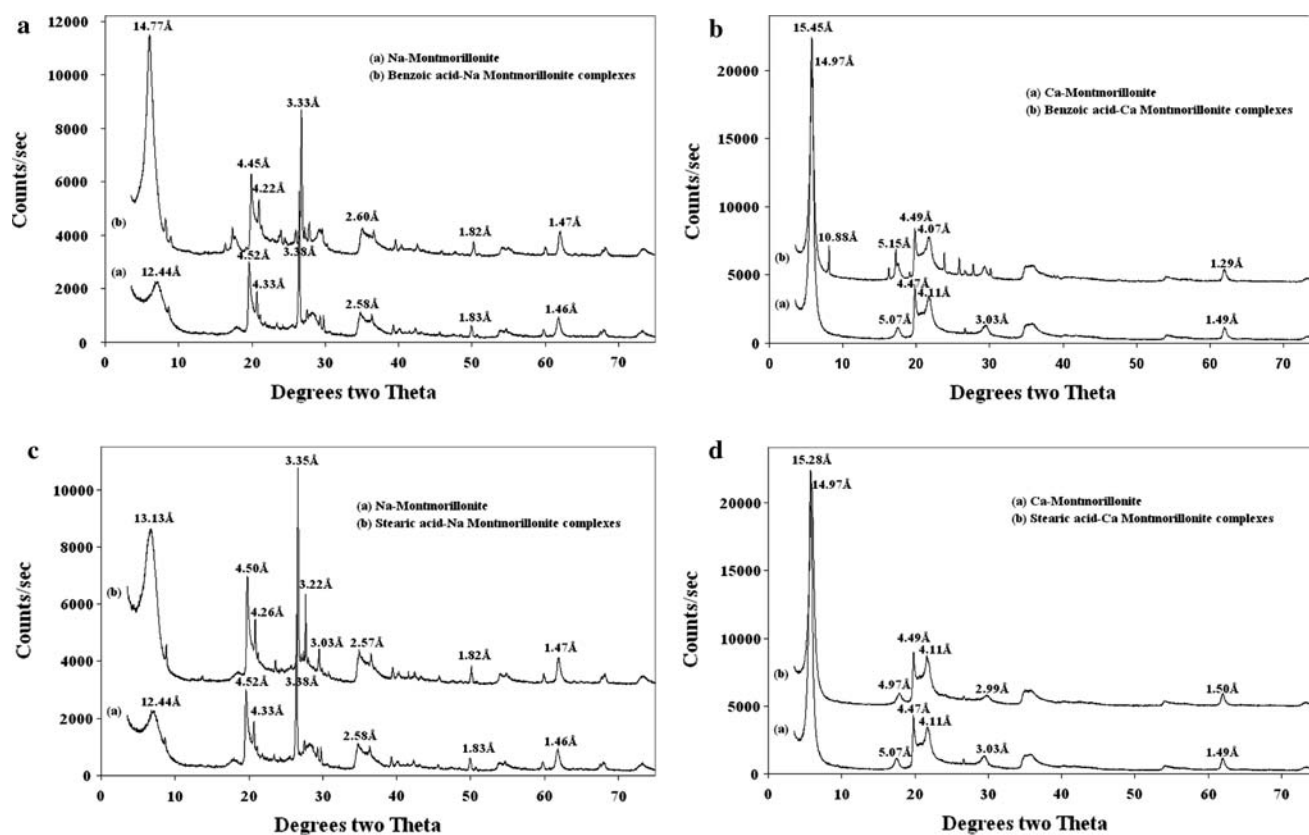


Fig. 1 X-ray diffraction of (a) sodium montmorillonite and benzoic acid adsorbed on sodium montmorillonite, (b) calcium montmorillonite and benzoic acid adsorbed on calcium montmorillonite, (c) sodium montmorillonite and stearic acid adsorbed on sodium montmorillonite and (d) calcium montmorillonite and stearic acid adsorbed on calcium montmorillonite

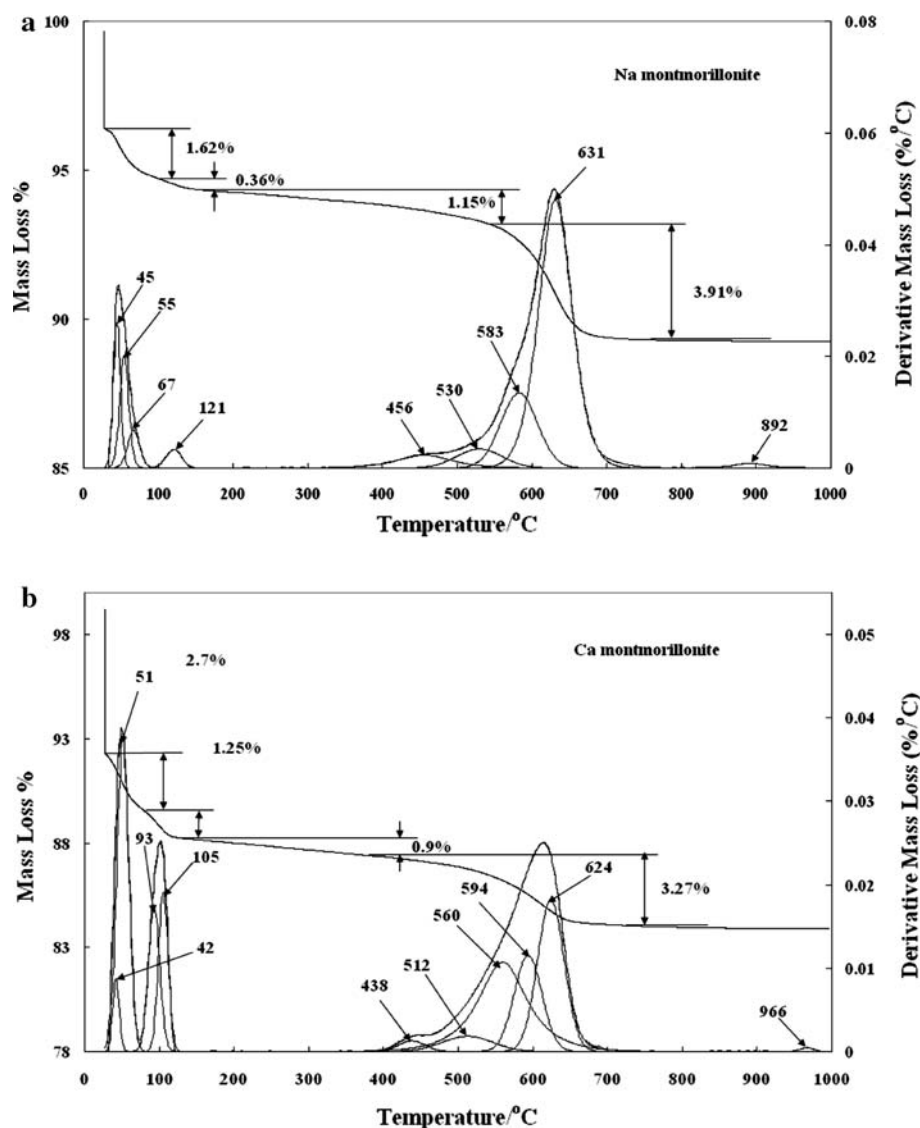
peak at 2θ value of 7.1° of sodium montmorillonite corresponding to 12.44 \AA shifted to 6.7° after adsorption stearic acid and to 5.9° after adsorption benzoic acid. The d_{001} spacing of stearic acid–sodium montmorillonite complexes increased to 13.13 \AA and benzoic acid–sodium montmorillonite complexes increased to 14.77 \AA , resulting from carboxylic acid intercalated into the sodium montmorillonite. The expansion of the sodium montmorillonite with benzoic acid and stearic acid is 2.33 and 0.69 \AA . The expansion of the calcium montmorillonite with benzoic acid and stearic acid is 0.48 and 0.31 \AA . The reason for the increased expansion of the NM with benzoic acid is attributed to (a) adsorption on the inner surfaces of the montmorillonite interlayer and (b) the structural arrangement of the benzoic acid molecules in the interlayer. The molecules are not layering flat to the surface but are at an angle to the inner surfaces.

Thermal analysis

The thermogravimetric analysis of sodium montmorillonites and calcium montmorillonite are shown in Fig. 2a and b. The DTG peak shows asymmetry on the higher

temperature side. This indicates that the hydroxyls may not be all lost simultaneously [46]. For the sodium (NM) and calcium montmorillonites (CM), two mass loss steps are observed centered at temperature ranges between 40 and $120 \text{ }^\circ\text{C}$ and 450 – $700 \text{ }^\circ\text{C}$. The first mass loss step is attributed to dehydration of the montmorillonites. The second mass loss step is due to dehydroxylation of the montmorillonite. The NM shows mass losses at 45 and $121 \text{ }^\circ\text{C}$ attributed to adsorbed water and water of hydration of the sodium cation in the montmorillonites interlayer. Mass losses of 1.62% and 0.36% are observed for these two dehydration steps. The distinction between the two dehydration steps is accentuated for the CM. The two mass loss steps occur at 51 and $105 \text{ }^\circ\text{C}$ with mass losses of 2.7% and 1.25% . The dehydroxylation of NM occurs over a wide temperature range from 400 to $700 \text{ }^\circ\text{C}$. Mass loss steps are observed at 456 , 530 , 583 and $631 \text{ }^\circ\text{C}$ and are attributed to dehydroxylation steps. The total mass loss for dehydroxylation is 4.1% . The dehydroxylation of CM occurs over a wide temperature range from 380 to $700 \text{ }^\circ\text{C}$. Mass loss steps are observed at 438 , 512 , 560 , 594 and $624 \text{ }^\circ\text{C}$ and are attributed to dehydroxylation steps. The total mass loss for dehydroxylation is 3.27% .

Fig. 2 Thermogravimetric and differential thermogravimetric analysis of (a) sodium montmorillonites and (b) calcium montmorillonite

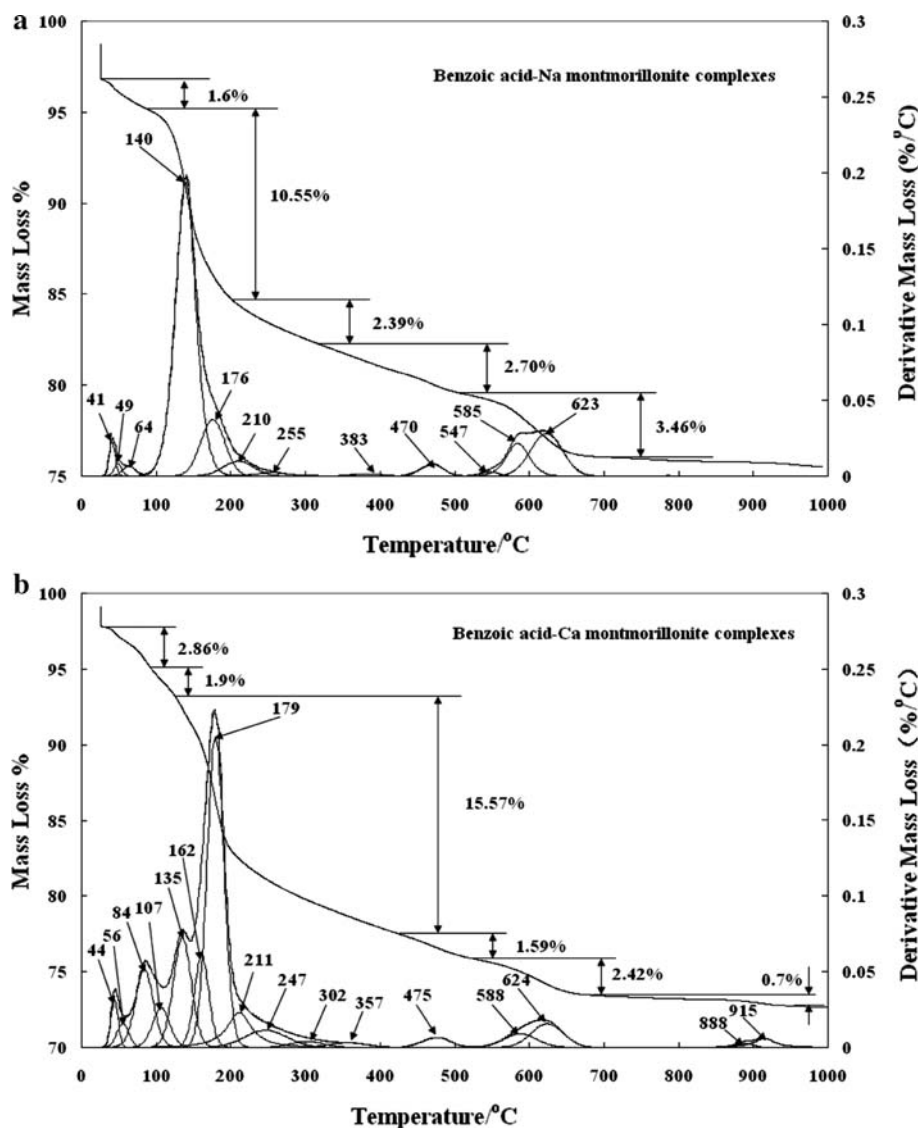


The thermogravimetric analysis through desorption of benzoic acid from benzoic acid adsorbed upon montmorillonites through thermal treatment are reported in Fig. 3a and b. The mass loss steps are observed over the 40–64 °C temperature range, over the 100–255 °C temperature range and in the 380–650 °C range. These mass loss steps are assigned to dehydration, sublimation of the benzoic acid combined with loss of water of hydration from the sodium ion, and dehydroxylation of the montmorillonite. A large mass loss is observed at 140 °C of 10.55%. Thus, the desorption of benzoic acid occurs from NM at significantly low temperatures. A comparison between Figs. 2a and 3a shows the DTG pattern in the 400–650 °C range is different for the benzoic acid adsorbed upon NM. It is proposed that the benzoic acid not only adsorbs on the surface of the montmorillonites but chemically reacts with the NM. It is possible that the carboxylic acid (–COOH) part of the

benzoic acid reacts with the siloxane surface of the montmorillonite and thus provides a mechanism for the loss of the inner hydroxyl group. The thermal treatment of the CM sample results in a series of mass loss steps at 44, 84, 135 and 179 °C assigned to dehydration of the CM and to the sublimation of the benzoic acid. It is noted that the benzoic acid sublimation occurs at higher temperatures for the CM compared with that of NM. This increase in temperature may be explained by the benzoic acid bonding to the calcium in the interlayer.

The thermal decomposition of stearic acid, as shown in Fig. 4a occurs at 176 °C. The thermal decomposition of stearic acid adsorbed on NM and CM are shown in Fig. 4b and c. Three distinct mass loss steps are observed for the thermogravimetric analysis of stearic acid adsorbed NM over the 46–115 °C temperature range, 200–400 °C temperature range and 500–700 °C temperature range. The first

Fig. 3 Thermogravimetric and differential thermogravimetric analysis of (a) sodium montmorillonite and (b) calcium montmorillonite with adsorbed benzoic acid

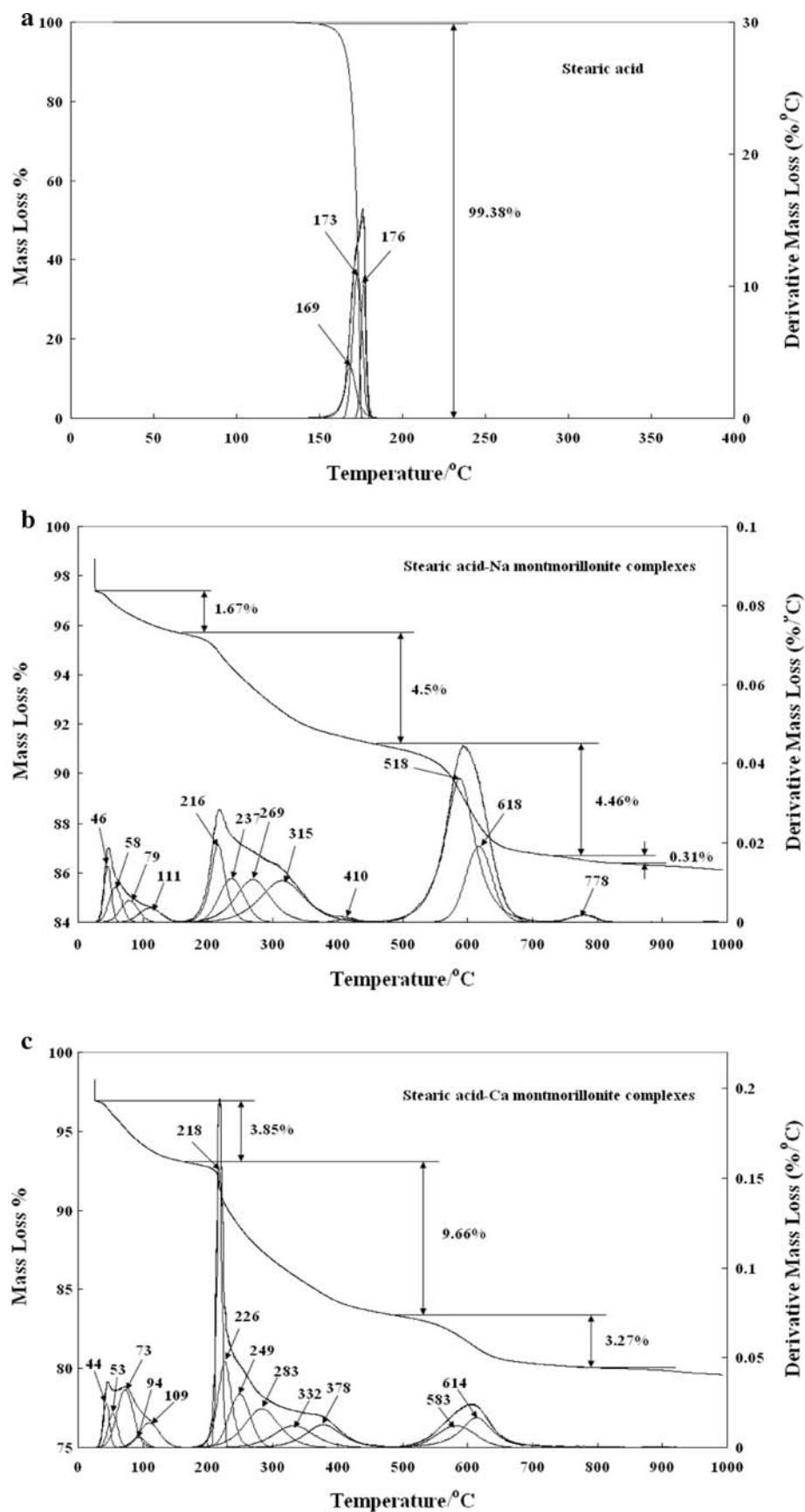


DTG set of peaks is assigned to dehydration; the second principally to sublimation of the stearic acid; and the third DTG peak to the dehydroxylation of the NM. It is noted that the dehydroxylation temperature is decreased to 518 °C through stearic acid adsorption. It is proposed that this decrease in DTG temperature of dehydroxylation provides evidence for a mechanism involving benzoic acid for the removal of the hydroxyl units from the montmorillonite. A similar set of results is observed for stearic acid adsorbed on CM. Three sets of DTG peaks are observed over the temperature ranges 40–115 °C, 200–380 °C and 500–700 °C temperature ranges. The large mass loss at 218 °C of 9.66% observed at 218 °C is ascribed to the sublimation of the stearic acid. The sublimation of the stearic acid occurs at higher temperatures than that for benzoic acid.

Conclusions

The desorption of the two common acids benzoic and stearic acid from sodium and calcium montmorillonites has been studied using a combination of thermogravimetric analysis and differential thermogravimetric analysis. Benzoic acid sublimates from the sodium montmorillonites at 140 °C and from the calcium montmorillonites at 179 °C. This difference in temperature is attributed to the differences in the chemisorptions of the benzoic acid on the sodium and calcium montmorillonites. This chemisorptions also affect the dehydroxylation of the montmorillonites which is lowered by the adsorption of the benzoic acid. It is proposed that the carboxylic acid (–COOH) part of the benzoic acid interacts with the siloxane surface of the

Fig. 4 Thermogravimetric and differential thermogravimetric analysis of (a) stearic acid, (b) sodium montmorillonite and (c) calcium montmorillonite with adsorbed stearic acid



montmorillonite and provides a mechanism for the loss of the inner hydroxyl group.

Acknowledgements The financial and infra-structure support of the Queensland University of Technology Inorganic Materials Research Program is gratefully acknowledged. The Australian Research Council (ARC) is thanked for funding the Thermal Analysis Facility. Financial supports from the National Natural Science Foundation of China through Grant Nos: 40672085 and 40872089) is acknowledged.

References

- Kennedy MJ, Pevear DR, Hill RJ. Mineral surface control of organic carbon in black shale. *Science*. 2002;295:657–60.
- Greene-Kelly R. Sorption of aromatic organic compounds by montmorillonite. I. Orientation studies. *Trans Faraday Soc*. 1955; 51:412–24.
- Greenland DJ, Laby RH, Quirk JP. Adsorption of amino acids and peptides by montmorillonite and illite. I. Cation exchange and proton transfer. *Trans Faraday Soc*. 1965;61:2013–23.
- Heller-Kallai L, Aizenshtat Z, Miloslavski I. The effect of various clay minerals on the thermal decomposition of stearic acid under 'bulk flow' conditions. *Clay Miner*. 1984;19:779–88.
- Sieskind O, Ourisson G. Clay-organic matter interactions. Formation of complexes between montmorillonite and stearic and behenic acids. *Comptes Rendus des Seances de l'Academie des Sciences, Serie C: Sciences Chimiques*. 1971;272:1885–8.
- Yan L-G, Wang J, Yu H-Q, Wei Q, Du B, Shan X-Q. Adsorption of benzoic acid by CTAB exchanged montmorillonite. *Appl Clay Sci*. 2007;37:226–30.
- Yariv S, Lapides I. The effect of mechanochemical treatments on clay minerals and the mechanochemical adsorption of organic materials onto clay minerals. *J Mater Synth Process*. 2000;8:223–33.
- Adu-Wusu K, Whang JM, McDevitt MF. Modification of clay-based waste containment materials, Conference proceedings—international containment technology conference, St. Petersburg, FL, Feb 9–12, 1997. p. 665–671.
- Akcaay G, Yurdakoc K. Removal of various phenoxyalkanoic acid herbicides from water by organo-clays. *Acta Hydrochim Hydrobiol*. 2000;28:300–4.
- Alther GR. Organoclay filtration technology for oil removal. *Adv Filtr Sep Technol*. 1999;13B:945–52.
- Alther GR. Organoclays remove humic substances from water. *Spec Publ R Soc Chem*. 2000;259:277–88.
- Alther G. Soil and groundwater remediation with organoclay. *Contam Soils*. 2001;6:225–31.
- Bhatt J, Bhalala BT. Use of organo-clay for decolorizing colored wastewater from the textile industry. *Vijnana Parishad Anusandhan Patrika*. 1995;38:249–54.
- Alther GR. Stormwater treatment. *Water Environ Technol*. 2001;13:31–4.
- Alther GR. Removal of emulsified oil from wastewater. *Fluid/Part Sep J*. 2000;13:146–51.
- Srinivasan KR, Fogler HS. Use of inorgano-organo-clays in industrial wastewater treatment. *Organohalogen Compd*. 1990;3: 417–20.
- Springman K, Mayura K, McDonald T, Donnelly KC, Kubena LF, Phillips TD. Organoclay adsorption of wood-preserving waste from groundwater. Analytical and toxicological evaluations. *Toxicol Environ Chem*. 1999;71:247–59.
- Brixie JM, Boyd SA. Treatment of contaminated soils with organoclays to reduce leachable pentachlorophenol. *J Environ Qual*. 1994;23:1283–90.
- Cruz-Guzman M, Celis R, Hermosin MC, Cornejo J. Sorption of the herbicide simazine by biomolecule-modified clays, Pesticide in Air, Plant, Soil & Water System, Proceedings of the Symposium Pesticide Chemistry, 12th, Piacenza, Italy, June 4–6, 2003. p. 185–191.
- Carrizosa MJ, Hermosin MC, Koskinen WC, Cornejo J. Use of organosmectites to reduce leaching losses of acidic herbicides. *Soil Sci Soc Am J*. 2003;67:511–7.
- Sand ID, Piner RL, Gilmer JW, Owens JT. Organoclays as processing aids for plasticized thermoplastics. USA: U.S. Eastman Chemical Company, Us; 2003. 8 pp.
- Rafailovich M, Si M, Goldman M. Flame retardant and UV absorptive polymethylmethacrylate nanocomposites. *PCT Int. Appl. USA: The Research Foundation of State University of New York; Wo*, 2003. 34 pp.
- Meinke O, Hoffmann B, Dietrich C, Friedrich C. Viscoelastic properties of polystyrene nanocomposites based on layered silicates. *Macromol Chem Phys*. 2003;204:823–30.
- Maiti P, Yamada K, Okamoto M, Ueda K, Okamoto K. New poly(lactide)/layered silicate nanocomposites: role of organoclays. *Chem Mater*. 2002;14:4654–61.
- Chaiko D. Preparation of organoclays with improved dispersibility from smectites and kaolin clays by coating clays with water-soluble polymer. *PCT Int. Appl. USA: University of Chicago; Wo*, 2002. 24 pp.
- Nzengung VA. Organoclays as sorbents for organic contaminants in aqueous and mixed-solvent systems. GA: Georgia Institute Technology, FIELD URL; 1993. 191 pp.
- Soule NM, Burns SE. Effects of organic cation structure on behavior of organobentonites. *J Geotech Geoenviron Eng*. 2001;127:363–70.
- Earnest CM. Characterization of smectite clay minerals by differential thermal analysis and thermogravimetry. Part I. Montmorillonite. *Perkin-Elmer Thermal Analysis Application Study* 31, Pt. 1; 1980. 8 pp.
- Yariv S. Differential thermal analysis (DTA) in the study of thermal reactions of organo-clay complexes. *Natural and Laboratory-Simulated Thermal Geochemical Processes*; 2003. p. 253–296.
- Yariv S. The role of charcoal on DTA curves of organo-clay complexes: an overview. *Appl Clay Sci*. 2004;24:225–36.
- Yariv S, Ovadyahu D, Nasser A, Shuali U, Lahav N. Thermal analysis study of heat of dehydration of tributylammonium smectites. *Thermochim Acta*. 1992;207:103–13.
- Pramoda KP, Liu T, Liu Z, He C, Sue H-J. Thermal degradation behavior of polyamide 6/clay nanocomposites. *Polym Degrad Stab*. 2003;81:47–56.
- Carmody O, Frost R, Xi Y, Kokot S. Selected adsorbent materials for oil-spill cleanup. A thermoanalytical study. *J Therm Anal Calorim*. 2008;91:809–16.
- Frost RL, Locke A, Martens WN. Thermogravimetric analysis of wheatleyite $\text{Na}_2\text{Cu}^{2+}(\text{C}_2\text{O}_4)_2 \cdot 2\text{H}_2\text{O}$. *J Therm Anal Calorim*. 2008;93:993–7.
- Frost RL, Locke AJ, Hales MC, Martens WN. Thermal stability of synthetic aurichalcite. Implications for making mixed metal oxides for use as catalysts. *J Therm Anal Calorim*. 2008;94:203–8.
- Frost RL, Locke AJ, Martens W. Thermal analysis of beaverite in comparison with plumbojarosite. *J Therm Anal Calorim*. 2008;92:887–92.
- Frost RL, Wain D. A thermogravimetric and infrared emission spectroscopic study of alunite. *J Therm Anal Calorim*. 2008;91:267–74.
- Hales MC, Frost RL. Thermal analysis of smithsonite and hydrozincite. *J Therm Anal Calorim*. 2008;91:855–60.
- Palmer SJ, Frost RL, Nguyen T. Thermal decomposition of hydrotalcite with molybdate and vanadate anions in the inter-layer. *J Therm Anal Calorim*. 2008;92:879–86.

40. Vagvolgyi V, Daniel LM, Pinto C, Kristof J, Frost RL, Horvath E. Dynamic and controlled rate thermal analysis of attapulgite. *J Therm Anal Calorim.* 2008;92:589–94.
41. Vagvolgyi V, Hales M, Frost RL, Locke A, Kristof J, Horvath E. Conventional and controlled rate thermal analysis of nesquehonite $\text{Mg}(\text{HCO}_3)(\text{OH}) \cdot 2(\text{H}_2\text{O})$. *J Therm Anal Calorim.* 2008;94:523–8.
42. Vagvolgyi V, Daniel LM, Pinto C, Kristof J, Frost RL, Horvath E. Dynamic and controlled rate thermal analysis of attapulgite. *J Therm Anal Calorim.* 2008;92:589–94.
43. Vagvolgyi V, Frost RL, Hales M, Locke A, Kristof J, Horvath E. Controlled rate thermal analysis of hydromagnesite. *J Therm Anal Calorim.* 2008;92:893–7.
44. Vagvolgyi V, Hales M, Martens W, Kristof J, Horvath E, Frost RL. Dynamic and controlled rate thermal analysis of hydrozincite and smithsonite. *J Therm Anal Calorim.* 2008;92:911–6.
45. Zhao Y, Frost RL, Vagvolgyi V, Waclawik ER, Kristof J, Horvath E. XRD, TEM and thermal analysis of yttrium doped boehmite nanofibres and nanosheets. *J Therm Anal Calorim.* 2008;94:219–26.
46. Kristof J, Frost RL, Kloprogge JT, Horvath E, Mako E. Detection of four different OH-groups in ground kaolinite with controlled-rate thermal analysis. *J Therm Anal Calorim.* 2002;69:77–83.